
Article:
Shi, P orcid.org/0000-0001-5782-245X, Yuan, S, Wang, T et al. (2 more authors) (2018) Fracture Identification in a Tight Sandstone Reservoir: A Seismic Anisotropy and Automatic Multisensitive Attribute Fusion Framework. IEEE Geoscience and Remote Sensing Letters, 15 (10). pp. 1525-1529. ISSN 1545-598X

https://doi.org/10.1109/LGRS.2018.2853631

Fracture Identification in a Tight Sandstone Reservoir: A Seismic Anisotropy and Automatic Multi-Sensitive Attribute Fusion Framework

Peidong Shi, Sanyi Yuan, Tieyi Wang, Yanyan Wang, and Tao Liu

***Abstract*—Fracture monitoring is crucial for many geo-industrial applications, such as carbon dioxide storage and hydrocarbon exploration in tight reservoirs, because fractures can form storage space or leaking paths for geological sealing. We propose a fracture identification framework for geo-industrial applications by exploiting seismic reflection anisotropy and automatic multi-sensitive attribute fusion. Anisotropy maps extracted from different seismic attributes are automatically selected and fused according to the correlation between the predicted anisotropy strengths and the measured fracture densities at well locations. Through seismic anisotropy extraction and automatic multi-sensitive attribute fusion, we can acquire a more comprehensive evaluation of different fracture types in a reservoir. The proposed fracture identification framework is successfully applied to a deep, tight sandstone reservoir in southwest China. The predicted fracture distribution is closely related to the local structures in the target reservoir. The orientations of most predicted fractures are consistent with the local maximum principal stress direction in this area, which is good for the opening and fluid filling of fractures. The fracture identification results will be used to guide hydrocarbon exploration activities in this region, such as exploration well deployment.**

***Index Terms*—Fracture identification, seismic anisotropy, tight sandstone, seismic attribute fusion, sensitive attribute selection.**

I. Introduction

TIGHT reservoirs, such as those comprising tight sandstone or shale, have played an increasing important role in hydrocarbon production. However, the permeability and porosity are often very low in tight reservoirs, which is not conducive to the storage and migration of oil and natural gas. Fractures play a key role in enhancing the permeability and porosity of tight reservoirs. Fractures can exist in nature or be induced by hydraulic fracturing [1], [2]. The fracture-rich areas are often the sweet spots for hydrocarbon exploration in tight reservoirs. Monitoring the distribution and growth of fractures in tight rocks is also very important for other geo-industrial applications, such as carbon dioxide storage (CCS) and nuclear waste disposal [3]. Natural or induced fractures can be ideal sealing sites for CCS, and conversely, they can result in leakage risks in geological waste disposal.

When seismic waves propagate through rocks with abundant aligned fractures, seismic anisotropy phenomena have been observed [4]. Seismic anisotropy techniques have been used to identify the properties of fractures, such as orientation and density [5]. The subsurface medium with lots of vertically aligned fractures can be equivalent to horizontal transverse isotropic (HTI) medium. The reflection anisotropy of HTI medium has been studied and used to identify the fracture distribution and elastic parameters of cracked medium with vertical fractures [6]. However, conventional fracture inversion methods using seismic reflection data have demanding requirements for data acquisition and are often unstable in the presence of noise. When the quality of the acquired data is low or the acquisition aperture is limited, the inversion results of these methods are normally unsatisfactory. In addition, these methods are limited to utilizing seismic amplitudes for identifying subsurface fractures, and cannot effectively use all of the acquired seismic data information.

Seismic attribute analysis has been introduced to help us extract geological features or reservoir properties from seismic data [7]–[9]. Different seismic attributes are sensitive to different reservoir properties or geological structures. For fracture identification, different seismic attributes characterize different aspects of fractures and/or different fracture types. Seismic anisotropy techniques, which are based on associated seismic attributes is also utilized to reveal fracture properties from different aspects [10]. In this paper, we introduce a fracture identification framework based on seismic anisotropy and multi-sensitive attribute fusion. The seismic anisotropy extracted from different seismic attributes are automatically selected and fused to better reveal the subsurface fractures. The proposed framework is successfully applied to a deep, tight sandstone reservoir. First, we describe the theory of fracture identification and integrate the whole workflow with automatic multi-sensitive attribute fusion. Then, we apply the fracture identification workflow to both synthetic and tight sandstone reservoir datasets. Finally, the fracture identification results of the tight sandstone reservoir are displayed and analyzed in detail. Through synthetic and real data examples, we demonstrate that the proposed fracture identification framework is a highly efficient and stable method and can effectively utilize the seismic data information from different aspects through automatic attribute fusion.

Manuscript received December 18, 2017; revised **** **, 2018. *(Corresponding author: Sanyi Yuan.)*

P. Shi is with the State Key Laboratory of Petroleum Resources and Prospecting, China University of Petroleum, Beijing 102249, China, and also with the School of Earth and Environment, University of Leeds, Leeds LS2 9JT, UK.

S. Yuan and T. Wang are with the State Key Laboratory of Petroleum Resources and Prospecting, China University of Petroleum, Beijing 102249, China (e-mail: yuansy@cup.edu.cn).

Y. Wang is with the Department of Earth Sciences, ETH Zurich, Zurich 8092, Switzerland.

T. Liu is with SINOPEC Petroleum Exploration & Production Research Institute, Beijing 100083, China.

II. METHODS

The reflection coefficient of the P-wave in the HTI medium is a function of the incident and azimuth angles [6]:

$$R_P^{HTI}(i,\phi) = \frac{\Delta Z}{2\overline{Z}} + \frac{1}{2}\left[\frac{\Delta\alpha}{\overline{\alpha}} - \left(\frac{2\overline{\beta}}{\overline{\alpha}}\right)^2 \frac{\Delta G}{\overline{G}}\right]\sin^2 i + \frac{1}{2}\left[\Delta\delta^v + 2\left(\frac{2\overline{\beta}}{\overline{\alpha}}\right)^2 \Delta\gamma\right]\sin^2 i\cos^2(\phi-\phi_{sym}) \tag{1}$$

where i and ϕ are the incident angle and azimuth angle of the incident P-wave, ϕ_{sym} is the azimuth angle of the symmetry axis of HTI medium, α and β is the vertical velocities of the P-wave and the fast S-wave, Z denotes the P-wave impedance, $G = \rho\beta^2$ denotes vertical shear modulus and ρ is bulk density, δ and γ are the Thomsen anisotropic parameters [11], which characterize the subsurface anisotropy. The HTI medium symmetry axis indicates the fracture plane orientation. High order terms about the incident angle have been neglected, which is often the case when the incident angle is small (e.g. $\leq 30°$).

Only the third term in (1) contains the subsurface anisotropic information. For weak anisotropy and a certain incident angle, the anisotropy ellipse can be used to characterize the azimuth distribution of reflected P-wave amplitudes [6]. Therefore, the ellipse fitting approach can be utilized to evaluate the anisotropy of the subsurface. For seismic data of different azimuths $\mathbf{d} = [d_1, d_2, \cdots, d_n]$ (n common reflection point (CRP) data of different azimuths), the ellipse distribution of the azimuth seismic data can be evaluated by minimizing an objective function:

$$min\ \mathbf{E}(\mathbf{d})_{obj} = \|\mathbf{AP} - \mathbf{B}\|_2^2 + \lambda\|\mathbf{P}\|_2^2 \tag{2}$$

where

$$\mathbf{P} = \begin{pmatrix} \frac{V}{U} & \frac{W}{U} & \frac{-1}{U} \end{pmatrix}^T$$
$$\mathbf{A} = \begin{pmatrix} d_1^2\sin^2\phi_1 & d_1^2\sin\phi_1\cos\phi_1 & 1 \\ d_2^2\sin^2\phi_2 & d_2^2\sin\phi_2\cos\phi_2 & 1 \\ \cdots & \cdots & \cdots \\ d_n^2\sin^2\phi_n & d_n^2\sin\phi_n\cos\phi_n & 1 \end{pmatrix} \tag{3}$$
$$\mathbf{B} = -\begin{pmatrix} d_1^2\cos^2\phi_1 & d_2^2\cos^2\phi_2 & \cdots & d_n^2\cos^2\phi_n \end{pmatrix}^T.$$

The solution $\mathbf{P}$ which is composed of U, V and W, contains the detailed information about the anisotropy ellipse. Once $\mathbf{P}$ is solved, we can calculate the lengths of the major and minor axes of the anisotropy ellipse and the directions of the major and minor axes of the anisotropy ellipse by using combinations of U, V and W. λ is a regularization parameter (normally a small value) and is used to improve the inversion stability and noise resistance. In these equations, azimuth angle ϕ_i (azimuth angle of the ith CRP data) is measured counterclockwise along the east direction. Because there are three unknown parameters in $\mathbf{P}$, we need seismic data from at least three different azimuths to solve the inverse problem. By solving the objective function, we can obtain the anisotropy ellipse of a specific reflection point in the subsurface:

$$\mathbf{P} = (\mathbf{A}^T\mathbf{A} + \lambda\mathbf{I})^{-1}\mathbf{A}^T\mathbf{B}. \tag{4}$$

For fracture identification, fracture density and orientation are the two main aspects used to evaluate the reservoir's fracture distribution. Fracture density is the key to assessing the storage capacity of tight reservoirs, and the fracture orientation controls the connectivity and migration of oil and gas in tight reservoirs. The fracture density can be semi-quantitatively evaluated with the major and minor axes ratio of the fitting anisotropy ellipse. In a weak anisotropic medium, the fracture density and anisotropy strength show a significant positive correlation with the major and minor axes ratio of the fitting anisotropy ellipse. The fracture orientation can be determined using the major or minor axis direction of the fitting anisotropy ellipse. The choice of using a major or minor axis to represent the fracture orientation depends on the coefficient of the third term in (1). If the coefficient is larger than 0, the direction of the minor axis corresponds to the fracture orientation. Otherwise, the direction of the major axis corresponds to the fracture orientation. For HTI media with an isotropic overburden, the coefficient is usually a negative value. Thus, in this situation, the direction of the major axis is used to determine the fracture orientation.

Once (4) is solved, the major/minor axis direction and the major and minor axes ratio of the anisotropy ellipse are determined through the following equation:

$$C = \tan\phi_{axis} = \frac{U-V}{W} \pm \sqrt{\left(\frac{U-V}{W}\right)^2 + 1}$$
$$r_{ani} = \sqrt{\frac{V - C^2U}{U - C^2V}} \tag{5}$$

where ϕ_{axis} indicates the direction of the major or minor axis and r_{ani} is the ratio of the major axis to the minor axis of an anisotropy ellipse. The anisotropy ellipse fitting approach is a highly efficient and stable way to estimate the anisotropy and fracture distribution of reservoirs.

In practice, apart from the recorded seismic amplitudes, seismic attributes such as seismic attenuation and frequency attributes can also be used as inputs for the proposed fracture identification framework. Seismic amplitude attributes are often sensitive to the dimension and aspect ratio of fractures. Seismic attenuation and frequency attributes are sensitive to rock attenuation properties, and thus, they are often a good indication of fractures filled with fluids such as oil or nature gas. The inverted anisotropy results based on different types of inputs characterize different fracture features and can be automatically fused together to better indicate the fracture distribution and fluid filling. Finally, the fused fracture distribution map of the reservoir can be expressed as follows:

$$\mathbf{F} = \sum_{i=1}^{N} w_i\mathbf{r}_i \tag{6}$$

where $\mathbf{F}$ represents the fused fracture distribution map, $\mathbf{r}_i$ represents the predicted seismic anisotropy map based on the ith seismic attribute, w_i represents the weighting factor for the ith seismic attribute and N is the total number of seismic attributes used in the fracture identification. The weighting factors are the key to implementing the anisotropy map fusion and can be better evaluated by using prior information from

wells. Prior information from wells, e.g., measured fracture densities from imaging logging or hydrocarbon production, can be exploited to determine the weighting factors of different attributes. The weighting factors for different attributes are evaluated by examining the correlation between the predicted anisotropy strength of different attributes and the measured prior information at the well locations. The more wells we have, the better we can estimate the weighting factors for different seismic attributes. The calculation of the weighting factor can be expressed as follows:

$$W_i = \frac{\sum_x (r_i(x) - \overline{r_i(x)})(m(x) - \overline{m(x)})}{(N_w - 1)\sigma_{r_i}\sigma_m} \tag{7}$$

where W_i is the weighting factor for the ith seismic attribute, $r_i(x)$ is the predicted seismic anisotropy from the ith seismic attribute at well position x, $m(x)$ is the measured prior information at well position x, N_w is the number of wells, σ is the standard deviation of the corresponding data and the overlines denote averages. The weighting factor W_i has a value between $+1$ and -1, where ± 1 represents a total positive or negative linear correlation between the predicted seismic anisotropy from a corresponding seismic attribute and the measured prior information at the well locations, and 0 represents no linear correlation. The weighting factors, which have a good correlation with the measured prior information, are then selected and normalized:

$$w_i = \begin{cases} 0, & W_i \le p_t \\ W_i / \sum\limits_{W_i > p_t} W_i, & W_i > p_t \end{cases} \tag{8}$$

where p_t is a preset correlation threshold. Only those seismic attributes that have higher correlation coefficients than the preset threshold are extracted and fused to form the final fracture distribution map. The weighting factors reflect the sensitivity of different attributes to the fractures and seismic anisotropy in this region. By utilizing the automatic weighting scheme, the sensitive attributes are automatically selected and fused to form the fracture distribution map, and the impact of human factors in attribute selection is thus eliminated. The whole fracture identification framework using seismic anisotropy and attribute fusion is shown in Fig. 1.

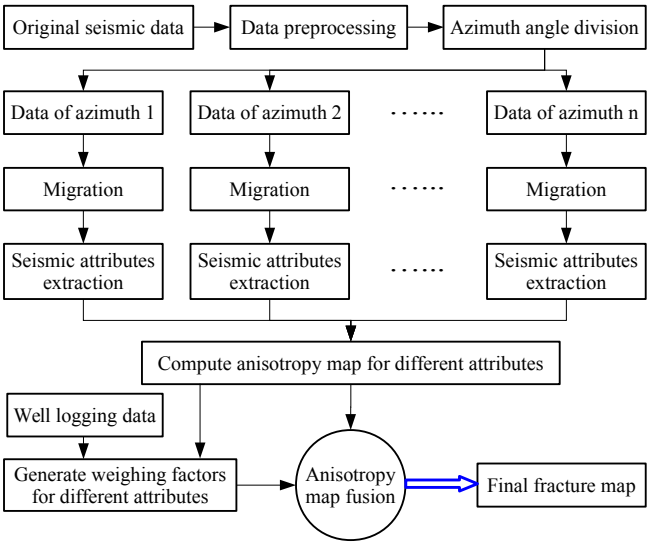

Fig. 1. Fracture identification framework using the seismic anisotropy and multi-sensitive attribute fusion technique.

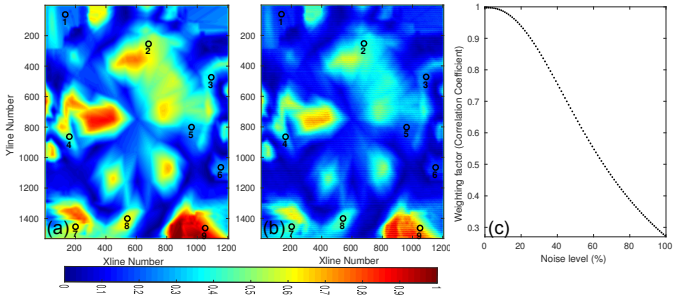

Fig. 2. (a) Relative anisotropic strength of the model. (b) Inverted anisotropic strength for the 20% random noise scenario. Black circles show the locations of nine virtual wells. (c) Variation in weighting factors with different noise levels.

III. Fracture Identification

A. Synthetic Data Example

To test and verify the effectiveness of the proposed fracture identification framework, we apply the method to a synthetic data example. A two-layered model is used to generate the synthetic dataset, where in the upper and lower layers, the P-wave velocities are 3724 m/s and 4640 m/s, the S-wave velocities are 1944 m/s and 2583 m/s and the densities are 2.45 g/cm^3 and 2.49 g/cm^3, respectively. The upper layer is an isotropic medium, while the lower layer is a HTI medium, with the relative anisotropic strength displayed in Fig. 2(a). The Thomsen anisotropic parameters in the HTI medium have the strongest values of δ=-0.05, ε=-0.05 and γ=-0.12. Seismic reflection data for the upper and lower layer interface are generated, and then, different levels of random noise are added. Fig. 2(b) shows the inverted anisotropic strength with 20% random noise added into the dataset. The inversion results can effectively represent the relative anisotropic strength of the model, which demonstrates that the proposed method is a stable and effective fracture identification technique. Nine virtual wells are settled and randomly distributed in the model (Fig. 2 black circles). Weighting factors (correlation coefficients) are then calculated using (7) for different noise levels (Fig. 2(c)). With an increase of noise levels, the weighting factors decrease accordingly. The weighting factors can be used to effectively evaluate the inversion results, which is the theoretical basis of the automatic multi-sensitive attribute fusion framework. In the synthetic example, we can only simulate the effect of different levels of noise to the inversion results. However, in practice, inversion results of different seismic attributes can have different sensitivity to subsurface fractures and can also reflect different fracture aspects, such as fluid filling and fracture aspect ratio. By using the weighting and attribute fusion, we can automatically select sensitive attributes and then effectively integrate the different sensitive results, finally obtaining a better fracture identification result.

B. Fracture Identification in a Tight Sandstone Reservoir

The research area is in southwest China, with an area of 150 km^2 (shown in Fig. 3(a)). The tectonic movement is very active in this area, which contributes to many faults, folds and fractures in the subsurface. Our target reservoir is located at depths of 4000-4500 m and has undergone compaction and densification processes. The reservoir is composed of tight sandstone, which has a very low porosity and permeability. However, considerable natural gas has been discovered in the target layer through the prospecting wells in the research area. The outcrops, core samples and imaging logging results show that massive vertical or near vertical fracture clusters are distributed in the target reservoir, where natural gases of commercial level have been discovered. Therefore, the fracture-rich zone of the target reservoir can be well approximated as HTI medium. To obtain the fracture distribution of the whole research area, a surface seismic monitoring array with a wide azimuth has been deployed and high quality seismic data are acquired. A recorded seismic reflection profile after processing is shown in Fig. 3(b). Geological interfaces are interpreted and picked up from the seismic data through seismic and well logging interpretations. Our target reservoir is between layers 4 (L4) and 5 (L5). The seismic data interpretation results indicate the existence of many faults in the subsurface, especially within the target reservoir. The faults further reveal active tectonic movements in this area, which may contribute to numerous fractures in the tight reservoir. Fig. 4 shows the azimuth and offset distribution of the seismic array. The offset coverage of the seismic data in different azimuths is uneven. To obtain reliable inversion results of the fracture distribution, we use seismic data with an offset range of 10 m to 3600 m to conduct the anisotropy inversion, where the offsets are evenly distributed in different azimuths. The seismic data are then divided into five groups with central azimuths of $14.2°$, $46.2°$, $90°$, $133.8°$ and $165.8°$, which is shown in Fig. 4.

The amplitude differences among azimuths due to seismic anisotropy are utilized to extract the anisotropy map and fracture distribution of the target reservoir. Apart from the original amplitude, we also extract 16 seismic attributes (e.g., total energy, instantaneous frequency, frequency attenuation gradient, etc., which can be divided into the seismic amplitude attribute, the seismic attenuation attribute and the seismic frequency attribute) to derive seismic anisotropy information. The seismic anisotropy maps of different attributes are correspondingly calculated based on these seismic attributes, and then are fused to form the final fracture distribution map. In our research, the weighting factors for different attributes are evaluated by examining the correlation between the predicted anisotropy strength and the measured fracture density at well locations. The correlation threshold (p_t) is set to 0.5. We only select the seismic attributes with correlation coefficients higher than 0.5 to form the final fracture map of the target layer.

The final fused anisotropy map for the top layer (L4) of the target reservoir is shown in Fig. 5. The predicted fracture clusters are mainly distributed around the fault and fold zones where the strata are bent, and the local structure is more complicated. In the tectonically active areas, such as the fault and fold zone, stress release can lead to the generation of a large amount of fractures. The coherence slice is also displayed and compared in Fig. 5. In overall, the fused anisotropy map is consistent with the classical coherence result, which confirms the reliability and effectiveness of the new method. Particularly, our result reveals much more details of the fracture distribution in the whole area, while the coherence result mainly shows the distribution of large scale faults. The predicted and measured fracture orientations at the well locations are also displayed and compared in Fig. 5. The predicted fracture orientations at a well location are obtained by counting the inverted fracture orientations within 600 m from the exact well location, which

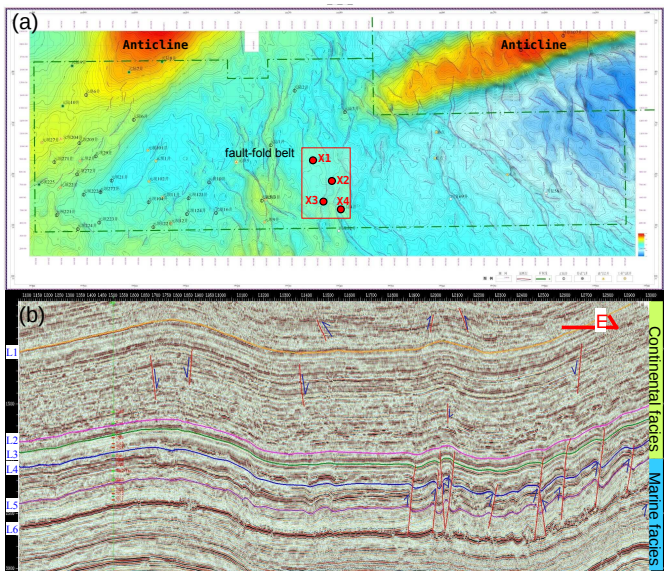

Fig. 3. (a) The topography of the target reservoir's top layer. The color represents the time depth extracted from the surface seismic reflection data. The faults and anticlines are shown on the map. The research area is marked by the red rectangle. Four prospecting wells have been deployed in the research area, which are highlighted by the red dots. Wells X1, X2 and X4 have a natural gas production of 22 k, 570 k and 23 k m^3/day in the target reservoir, respectively. (b) A recorded seismic profile after processing. Six layers have been recognized and picked up, with orange, pink, green, blue, purple and black lines showing the L1-L6 layers, respectively. The top and bottom layers of the target reservoir are L4 and L5. The faults have been interpreted and highlighted by red lines.

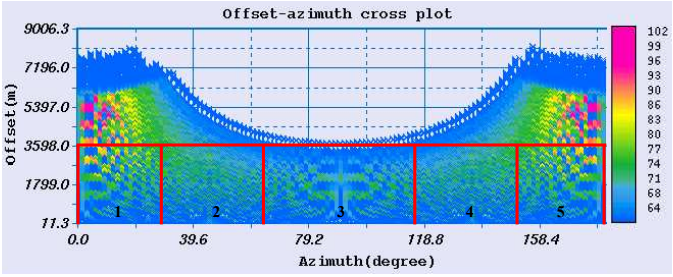

Fig. 4. The azimuth and offset crossplot of the monitoring array. The color bar shows the azimuth-offset pair coverage.

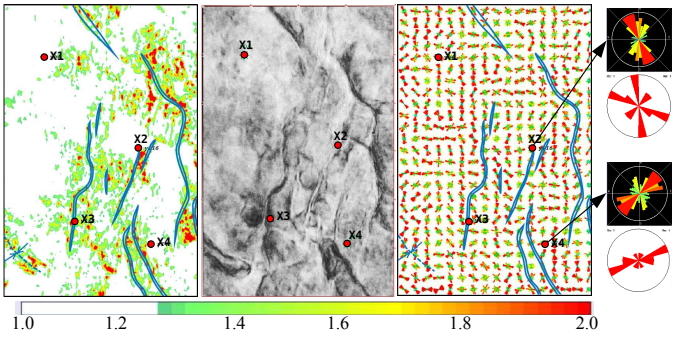

Fig. 5. The fused seismic anisotropy map for the top layer (L4) of the target reservoir. The left panel shows the predicted seismic anisotropy strength i.e., fracture density. The color represents the predicted relative fracture density, and the corresponding color bar is shown at the bottom. The middle panel shows a classical coherence slice of this layer. The right panel shows the predicted fracture orientation. The predicted fracture orientations (black box) through seismic anisotropy and the measured fracture orientations (white box) through imaging logging are also displayed and compared at two well locations. The blue solid lines show the interpreted fault polygon, and the blue dashed lines show the interpreted syncline.

are shown as rose diagrams (black box) in the Fig. 5. In the rose diagram, azimuth angles are divided into 36 groups (10° for each azimuth group), and the radial length represents the number of predicted fractures whose orientations fall into that specific azimuth group. Rose diagrams of the measured fracture orientations at the corresponding well locations (white box) represent the measured fracture orientations at the target layers, which are interpreted from the imaging logging data. For target layer L4, the measured fractures at well X4 have a dominant orientation of 70°-90°, and the predicted fractures have a dominant orientation of 40°-80°. Overall, the predicted fracture cluster orientations at the well locations correspond well with the measured fracture orientations from the imaging loggings, which further demonstrates the reliability of the results. Most predicted fracture clusters are orientated in the north-south direction or northwest-southeast direction, which is in accordance with the orientations of most faults in this area. The fracture clusters are abundant in the eastern part of our research area, whereas few fracture clusters are distributed in the northwestern part of the research area. According to the stress field information in this area and the orientations of the drilling-induced fractures, the maximum principal stress axis strikes nearly in the north-south direction or northwest-southeast direction. The direction of the maximum principal stress axis is in correspondence with the orientations of most predicted fractures, which is favorable for fracture opening.

IV. Conclusions

In this letter, we introduce a fracture identification framework by utilizing seismic anisotropy and an automatic multi-sensitive attribute fusion technique. The predicted anisotropy maps of different seismic attributes are obtained by anisotropic ellipse fitting, and are then automatically fused to form the final fracture distribution map. Because different seismic attributes show different sensitivities to fractures and characterize different fracture aspects in a reservoir, an automatic weighting and fusion scheme is applied in the fracture identification framework. The weighting factors for different attributes are automatically evaluated by a comparison with the prior well data information, such as the measured fracture densities at well locations. Through automatic multi-sensitive attribute fusion, we select the anisotropy maps of sensitive attributes and obtain a more comprehensive evaluation of the fracture distribution in the reservoir. Effective information e.g., seismic amplitude, attenuation and frequency in the acquired seismic data are jointly utilized for the inversion of subsurface fractures using the automatic attribute fusion. The new proposed framework needs prior well information, and thus is more applicable to research area which has many wells.

We apply the proposed fracture identification framework to a deep, tight sandstone reservoir in southwest China. The inversion results show that the fracture cluster distributions have a close relationship with the faults and folds in this region. In the structure-complicated area, the tectonic movement is active, which can result in abundant fracture generation. Most predicted fractures strike in the north-south or northwest-southeast direction, which is in accordance with the direction of the local maximum principal stress. The consistency of the fracture orientations and the directions of the local maximum principal stress is favorable for fracture opening. Therefore, the fracture abundance zone has great potential to be a gas abundant area (as confirmed by well X2, which has a natural gas production of 570 k m^3/day). The fracture identification results of the target reservoir provide guidance for future hydrocarbon exploration in this region.

References

[1] Q. Sun, R. Zhang, Q. Zhan, and Q. H. Liu, "Multiscale hydraulic fracture modeling with discontinuous galerkin frequency-domain method and impedance transition boundary condition," *IEEE Trans. Geosci. Remote Sens.*, vol. 55, no. 11, pp. 6566–6573, Aug. 2017.

[2] Y. Hu, Y. Fang, D. LaBrecque, M. Ahmadian, and Q. H. Liu, "Reconstruction of high-contrast proppant in hydraulic fractures with galvanic measurements," *IEEE Trans. Geosci. Remote Sens.*, Dec. 2017.

[3] S. M. Benson and T. Surles, "Carbon dioxide capture and storage: An overview with emphasis on capture and storage in deep geological formations," *Proc. IEEE*, vol. 94, no. 10, pp. 1795–1805, Nov. 2006.

[4] S. Crampin, "A review of wave motion in anisotropic and cracked elastic-media," *Wave motion*, vol. 3, no. 4, pp. 343–391, Oct. 1981.

[5] S. Wang, X.-Y. Li, Z. Qian, B. Di, and J. Wei, "Physical modelling studies of 3-D P-wave seismic for fracture detection," *Geophys. J. Int.*, vol. 168, no. 2, pp. 745–756, Feb. 2007.

[6] A. Rüger, *Reflection coefficients and azimuthal AVO analysis in anisotropic media*. Tulsa, OK, USA: SEG, 2002.

[7] S. Chopra and K. J. Marfurt, *Seismic attributes for prospect identification and reservoir characterization*. Tulsa, OK, USA: SEG, 2007.

[8] S. Wang, S. Yuan, B. Yan, Y. He, and W. Sun, "Directional complex-valued coherence attributes for discontinuous edge detection," *J. Appl. Geophys.*, vol. 129, pp. 1–7, Jun. 2016.

[9] S. Yuan, S. Wang, M. Ma, Y. Ji, and L. Deng, "Sparse bayesian learning-based time-variant deconvolution," *IEEE Trans. Geosci. Remote Sens.*, vol. 55, no. 11, pp. 6182–6194, Jul. 2017.

[10] R. A. Clark, P. M. Benson, A. J. Carter, and C. A. G. Moreno, "Anisotropic p-wave attenuation measured from a multi-azimuth surface seismic reflection survey," *Geophys. Prospect.*, vol. 57, no. 5, pp. 835–845, Sep. 2009.

[11] L. Thomsen, "Weak elastic anisotropy," *Geophysics*, vol. 51, no. 10, pp. 1954–1966, Oct. 1986.